Interfacial spectroscopic characterization of organic/ferromagnet hetero-junction of 3,4,9,10-perylene-teracarboxylic dianhydride-based organic spin valves

Jhen-Yong Hong,[1] Kui-Hon Ou Yang,[1] Bo-Yao Wang,[1,2] Kai-Shin Li,[1] Hung-Wei Shiu,[3] Chia-Hao Chen,[3] Yuet-Loy Chan,[3] Der-Hsin Wei,[3] Fan-Hsiu Chang,[3] Hong-Ji Lin,[3] Wen-Chung Chiang,[4,a)] and Minn-Tsong Lin[1,5,b)]
[1]*Department of Physics, National Taiwan University, 10617 Taipei, Taiwan*
[2]*Department of Physics, National Changhua University of Education, Changhua 500, Taiwan*
[3]*National Synchrotron Radiation Research Center, 30076 Hsinchu, Taiwan*
[4]*Department of Physics, Chinese Culture University, 11114 Taipei, Taiwan*
[5]*Institute of Atomic and Molecular Sciences, Academia Sinica, 10617 Taipei, Taiwan*

(Received 31 October 2013; accepted 3 February 2014; published online 24 February 2014)

We report interfacial characterization of 3,4,9,10-perylene-teracarboxylic dianhydride (PTCDA)-based organic spin valves (OSV) dusted with a thin layer of partially oxidized alumina at the organic semiconductor (OSC)/ferromagnet (FM) interfaces. Up to 13.5% magnetoresistance is achieved at room temperature. X-ray photoelectron spectroscopy measurements reveal interfacial electronic interaction between PTCDA and FM while the application of a thin alumina layer at the PTCDA/FM interfaces prevents the electronic hybridization and effectively preserves the spin injection into the OSC spacer. This finding demonstrates the critical effect of interfacial structure on magnetotransport behavior in OSV. © *2014 AIP Publishing LLC*.
[http://dx.doi.org/10.1063/1.4866164]

The efficient injection and transport of spin-polarized electrons into carbon-based materials have been a focus of attention in spintronics,[1] especially in the recently much-interested organic spintronics in which the control of injection and the detection of spin-polarized electrons via the organic semiconductor (OSC) barrier have been intensively investigated and significant progresses have been made.[2–7] Late technological reports have revealed the critical factors that influence the OSC-based spintronic device performance;[8–12] among them, the interface formed between the metallic and the OSC layers is proven an important key. This comes as no surprise because the changes in structure,[13] morphology,[8] density, and electronic structure[14,15] of an OSC thin film grown on different substrates have been demonstrated to impact its own transport properties. It has also been demonstrated that the charge transport in organic molecules is sensitively altered by the stacking direction of the molecules in organic thin-film transistors.[16,17] To improve the performance of molecular-level OSC-based spintronic devices, a thorough investigation of the correlation between the molecular orientation and the electronic structure as well as how the hetero-interface properties influence the efficiency of spin injection through the OSC layer needs to be carried out.

In a recent study we have conducted a series of experiments on organic spin valves (OSV) comprising a thin OSC barrier of 3,4,9,10-perylene-teracarboxylic dianhydride (PTCDA) dusted with partially oxidized alumina at the OSC/ferromagnet (FM) interface. Preliminary results can be found in a late publication in which an inelastic tunneling characteristic with 12% magnetoresistive (MR) effect has been reported. The device revealed real transport of spin-polarized electrons through the OSC material.[18] In the present work, we take a step further to address how the molecular orientation and the interfacial electronic structure of the FM/organic hetero-junction influence the MR performance of PTCDA-based organic spin valves. A 13.5% MR effect is achieved in these OSVs at room temperature. Angle-resolved Near Edge X-ray Absorption Fine Structure (NEXAFS) spectroscopic studies reveal that the PTCDA molecules align in an in-plane orientation with an effective contact angle of $12° \pm 3°$ to the substrate. X-ray Photoelectron Spectroscopy (XPS) measurements indicate that the direct contact of PTCDA molecules with the ferromagnetic Co underlayer results in a strong chemical interaction between Co and the single-bonded oxygen atom in PTCDA, leading to the formation of CoO that suppresses the efficient spin injection from Co into PTCDA. The insertion of a thin AlO_x layer into the FM/OSC interface effectively blocks the chemical interaction and hence the efficiency of the injection is preserved.

The PTCDA organic spin valves were constructed in the sequence of NiFe (25 nm)/Co (15 nm)/AlO_x (0.6 nm)/PTCDA (2 nm)/AlO_x (0.6 nm)/Co (30 nm) from bottom to top, in which the PTCDA was isolated from ambiance by the ferromagnetic electrodes. In between the OSC PTCDA spacer and the neighboring Co layers, a thin, partially oxidized alumina is inserted, as schematically shown in Fig. 1(a). The whole stack of sample was prepared in a high-vacuum environment using the same procedures as described in our recent work.[18] The Current-Perpendicular-to-the-Plane (CPP) resistances were obtained by the conventional four-point-probe method. The molecular orientation and the interfacial electronic properties of the OSC/FM interface were investigated on separate samples made intentionally without the top AlO_x layer and the capping Co electrode, but under identical conditions as the regular OSV samples, using NEXAFS spectroscopy at Beamline 05B2

a)Electronic mail: wchiang@faculty.pccu.edu.tw
b)Electronic mail: mtlin@phys.ntu.edu.tw

(fixed-angle) and Beamline 11A (angle-resolved), and XPS at Beamline 09A1, respectively, of National Synchrotron Radiation Research Center (NSRRC) in Taiwan. To reduce the impact of ambiance exposure, the samples were put into a vacuum container shortly after removing from the deposition chamber for transportation to NSRRC. The orbital orientation of the molecules was characterized in the total electron yield mode with a photon energy resolution of 0.1 eV according to the resonance correlation between the π^*-orbital of the molecules and the linear electric-field (E-field) polarization while the 0.12 eV XPS energy resolution was set by the pass energy of 5.85 eV in the Hemispherical Sector Analyzer (HSA). The XPS curves were synthesized by the convolution of Lorentzian and Gaussian contributions, i.e., the so-called Voigt profile, using the UNFIT simulation program.[19]

The cycling of junction resistance with field of a PTCDA-based OSV is shown in Fig. 1(b). The curve displays the typical pseudo spin-valve type characteristics at room temperature with an MR ratio of 13.5%, where the MR ratio is defined as

$$\frac{\Delta R}{R_P} = \frac{R_{AP} - R_P}{R_P}, \tag{1}$$

with R_P and R_{AP} indicating the resistances when the magnetizations of the FM electrodes are in the parallel and antiparallel configurations, respectively. The spin valve made without the insertion of AlO_x interlayers displays no MR effect. Fig. 1(c) shows the current-voltage (I–V) response curve of the same spin valve. The curve's nonlinear characteristic rules out the possible contribution of short-circuit channels within the device. The resistance-area product (RA value, which is in the order of $10^7\ \Omega \cdot \mu m^2$) is comparable to those reported in previous works.[4,18] The nonlinearity of the I–V curve, along with the proper RA value, evidence that the electric transport is occurring through the organic PTCDA spacer. Detailed spin transport mechanism of PTCDA spin valves has been characterized by inelastic electron tunneling spectroscopy and discussed in length in our previous study.[18]

Figures 2(a) and 2(b) show the polarization-dependent C and O K-edge NEXAFS spectra of 2 nm-thick PTCDA films deposited onto AlO_x/Co and directly onto Co, respectively. The two spectra are virtually indistinguishable because for PTCDA of 2 nm thickness, NEXAFS is insensitive to the interface underneath due to the limited mean free path of the outcoming electrons. Thus, NEXAFS is mainly used for the characterization of molecular orientation of PTCDA. The four sharp absorption peaks (A, B, C1, and C2) appearing in the C K-edge from 284 to 289 eV with p-polarized incident x-ray (black curve) exhibit the characteristic resonant transitions from the core levels of various carbon atoms into the unoccupied molecular orbitals of PTCDA. The first two peaks at 284.0 eV (peak A) and 285.4 eV (peak B) are attributed to the transitions from carbon atoms in the aromatic perylene core to the LUMOs whereas peak C1 (287.5 eV) and peak C2 (288.2 eV) are attributed to the transitions from carbon atoms within the anhydride functional groups to the LUMOs (see Table I for details).[20,21] As for the O K-edge spectra, the three distinct peaks (a, b, and c) also represent the resonant transitions of oxygen atoms within the anhydride functional groups into the LUMOs (see Table I).[20,22] According to the dipole selection rules, a transition to the unoccupied π^* (σ^*) orbital is allowed when the electric field vector $\vec{E}$ of the incident linearly polarized x-ray is parallel to the π^* (σ^*) orbital and is forbidden when $\vec{E}$ is perpendicular to the π^* (σ^*) orbital,[23] as schematically illustrated in the inset of Fig. 2(a). Our data show that the maximum intensity of the π^* resonance peaks A (a), B (b), and C (c) of the C K-edge (O K-edge) of PTCDA is observed with p-polarized incident x-ray whereas the minimum intensity is observed when the incident x-ray is s-polarized. For the planer PTCDA molecules, the π^* (σ^*) orbitals are pointing along

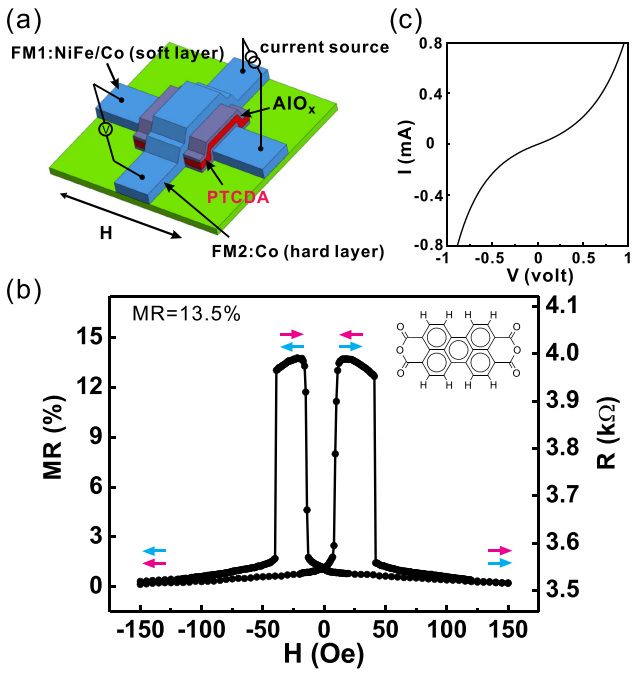

FIG. 1. (a) Schematic diagram of the tri-layered OSV dusted with partially oxidized alumina at the OSC/FM interfaces. (b) The room-temperature magnetoresistive curve of an OSV with 2 nm PTCDA spacer. The inset shows the chemical structure of PTCDA molecule. (c) The I-V curve of the PTCDA OSV.

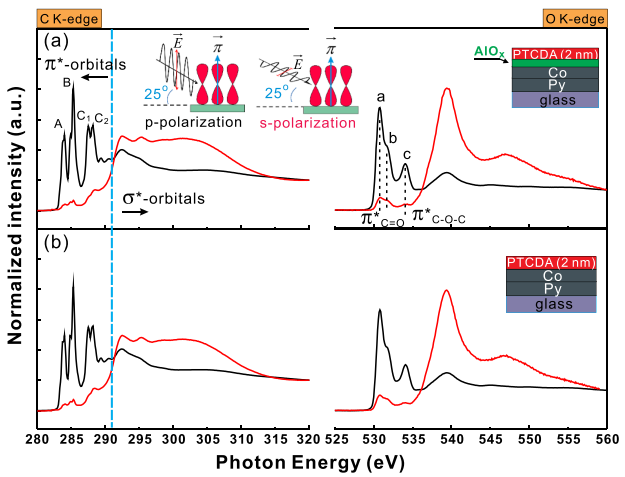

FIG. 2. Polarization-dependent C K-edge (left) and O K-edge (right) NEXAFS spectra of 2 nm PTCDA deposited onto (a) AlO_x/Co and (b) Co. The inset diagram displays the incident electric field vectors of p-polarized and s-polarized x-ray with respect to the π-orbital of PTCDA.

TABLE I. C K-edge and O K-edge NEXAFS characterization of PTCDA thin films as seen in Figs. 2 and 3.

Core hole atom	Peak	E (eV)	Assignment[22]
C	A	284.9	C_{C-H} 1S → LUMO
	B	285.4	$C_{perylene\ core}$ 1S → LUMO, LUMO+1
	C1	287.5	$C_{anhyd.}$ 1S → LUMO
	C2	288.2	$C_{anhyd.}$ 1S → LUMO+1
O	a	530.8	$O_{C=O}$ 1S → LUMO
	b	531.7	$O_{C=O}$ 1S → LUMO+1
	c	534.1	$O_{C=O}$ 1S → LUMO+3, O_{C-O-C} 1S → LUMO+1

the out-of-plane (in-plane) direction. Thus the PTCDA molecular plane (both perylene and anhydride groups) is essentially oriented in the lying-down configuration whether PTCDA is deposited onto AlO_x/Co or directly onto the Co underlayer.

Fig. 3 shows the angle-resolved O K-edge NEXAFS spectra (left column) and the variation of π^* resonance intensity at 530.8 eV (right column) of PTCDA as a function of x-ray incident angle θ recorded on the two types of samples discussed above (see Fig. 2). The intensity is obtained by integrating the peak area through curve fitting.[23,24] To account for the angle-dependent variation of absorption path and the collection efficiency, the spectra are normalized such that they coincide at photon energies far below (i.e., 525 eV) and far above (i.e., 560 eV) the O K-edge absorption edge. This procedure effectively normalizes the signal to the number of atoms sampled in the experiment. As seen in the right column of Fig. 3 (both (a) and (b)), the π^* resonance at 530.8 eV, which is due to the resonant transition from the O 1s core levels of the O=C bond in the anhydride functional groups into the unoccupied molecular orbitals of PTCDA, exhibits a maximum intensity at grazing incidence ($\theta \approx 10°$–$20°$). The intensity decreases with θ, reaching a minimum value at perpendicular incidence ($\theta = 90°$) and increases again as θ goes beyond 90°. In case any orientation disorder is present during the angular variation of x-ray incidence, the perfect perpendicularity between the electric field vector and the molecules cannot be established and thus no minimum intensity should be observed. The angular dependence of π^* resonance intensity reveals the average stacking orientation of PTCDA molecules. A quantitative analysis can be made by fitting this angular dependence using the following equation[23]

$$I_{\pi^*} = C[P(\cos^2\theta\cos^2\alpha + \sin^2\theta\sin^2\alpha\cos^2\phi + 2\sin\alpha\cos\alpha\sin\theta\cos\theta\cos\phi)] + C(1-P)(\sin^2\alpha\sin^2\phi), \quad (2)$$

where C and P are the normalization constant and the linear polarization factor (0.9), respectively, α is the average tilt angle of π^* vector orbital versus the surface normal, and ϕ is the azimuthal orientation of the molecules relative to the substrate. The fitting yields a tilt angle of 12° ± 3° for the average stacking orientation of the molecules with respect to the contact plane (either AlO_x or Co).

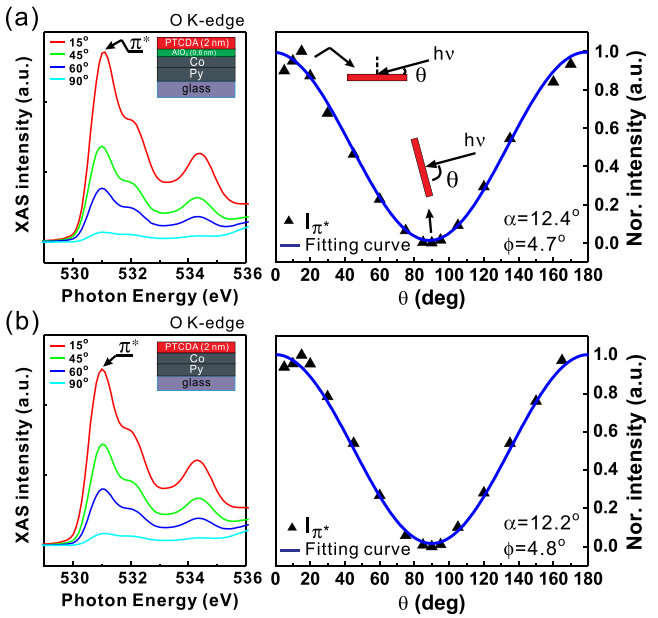

FIG. 3. Angle-resolved O K-edge NEXAFS spectra (left) and the integrated peak intensity of π^* resonance at 530.8 eV of PTCDA as a function of x-ray incident angle θ (right) recorded on 2 nm PTCDA deposited on (a) AlO_x/Co and (b) Co. The blue curves in the graphs at right represent the best fits using Eq. (2) described in the text.

The C 1s and O 1s core-level XPS spectra are shown in Figs. 4(a) and 4(b) for PTCDA deposited onto AlO_x/Co and Co, respectively. Since XPS is a relatively surface-sensitive technique with a typical probing depth less than ≈2 nm, the PTCDA films used for the XPS studies are intentionally made thinner at 1.25 nm instead of 2 nm. The main lines are curve fitted by the Voigt profiles using a constant Lorentzian line width of 0.08 eV (C 1s) and 0.12 eV (O 1s) and a variable width for the Gaussian contribution. In Fig. 4(a), the main peaks C1 and C2 in the C 1s spectrum at binding energies (BE) 284.7 eV and 285.2 eV represent the C-H bond and the sp^2-formed carbon (C=C) of the aromatic part in the perylene of PTCDA, respectively; whereas peak C3 at BE 288.8 eV stems from the carbon atoms in the anhydride part (O-C=O) of PTCDA.[25] As for the O 1s spectrum, the main peaks O1 (O=C) at 531.8 eV and O2 (C-O-C) at 533.5 eV are characteristics of PTCDA molecules.[25] Fig. 4(b) shows the C 1s and O 1s XPS spectra of PTCDA deposited directly on Co. Here the intensities of peak C3 and the other peaks for the π to π^* transition decrease and a new peak C′ is present which arises from the higher oxidation state of the perylene core. Meanwhile, the intensity of O2 peak in the O 1s spectrum decreases substantially accompanied by the rising signal of O-Co, indicating a strong interaction between the single-bonded O atoms (C-O-C) in the anhydride part of PTCDA and Co when the PTCDA molecules are attached directly onto the Co surface. To exclude the impact played by ambiance exposure, we also compare the O 1s spectra with that of a 2 nm PTCDA sample deposited on alumina(1 nm)/Co (made and transported under identical conditions). The spectra of 1.25 nm and 2 nm PTCDA on alumina resemble each other, with the main peaks for C=O and C-O-C retaining the characteristics of PTCDA, whereas the spectrum of 1.25 nm PTCDA on Co differs significantly, indicating that ambiance exposure is not a critical issue and what really matters is the underlayer material that

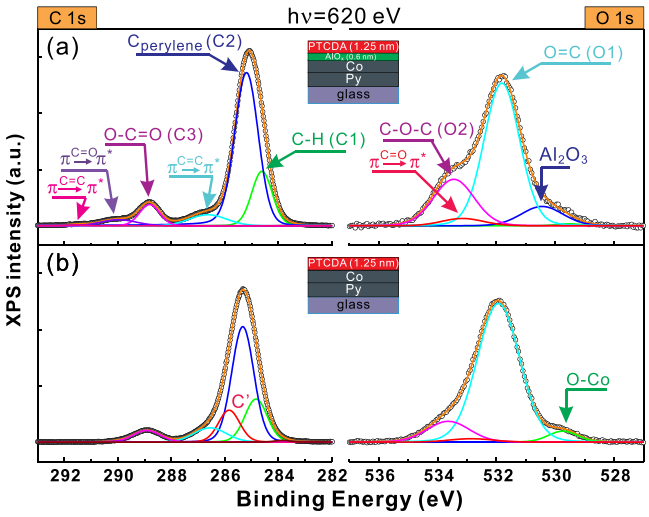

FIG. 4. The XPS C 1s and O 1s spectra of 1.25 nm PTCDA deposited onto (a) AlO_x/Co and (b) Co. The open circles indicate the measured XPS data whereas the orange curves are fitted lines obtained by superposition of individual components.

contacts PTCDA. It has been reported that the formation of a mixed oxidation layer upon the metal surface reacts with the anhydride (C-O) end groups of PTCDA when the metal is brought directly onto PTCDA.[26] The forming of Co-O hybridization at the FM/OSC interface, as seen in our sample with direct contact of PTCDA/Co, is likely to restrain efficient injection of spin-polarized electrons from FM into OSC and therefore suppress the performance of OSV. To prevent such hybridization and to retain effective spin injection into OSC, the application of a thin partially oxidized AlO_x barrier at the FM/OSC interface effectively reduces the electronic interaction between Co and PTCDA, as suggested by the XPS results of Fig. 4(a).

In summary, the organic PTCDA spin valve with the insertion of partially oxidized alumina at the OSC/FM interfaces achieves a room-temperature MR ratio of 13.5% in this study. The NEXAFS results show that the PTCDA molecules are essentially lying flat regardless of the underlayer (i.e., AlO_x/Co or Co) they are deposited onto, therefore the possibility that a different molecular orientation of PTCDA in the OSVs with AlO_x leads to the MR performance is precluded. The C 1s and O 1s core-level XPS spectra indicate the formation of a hybridized layer at the OSC/FM interface while the application of a thin AlO_x layer prevents the electronic interaction between Co and PTCDA and preserves effective spin injection into the organic PTCDA spacer. These results are beneficial to the understanding of interfacial electronic properties of OSC/FM hetero-junctions which are essential for designing future OSV-type spintronic devices.

This work was supported by the National Science Council of Taiwan under Grant No. NSC 100-2120-M-002-002.

[1]W. J. M. Naber, S. Faez, and W. G. van der Wiel, J. Phys. D: Appl. Phys. **40**, R205 (2007).
[2]V. Dediu, M. Murgia, F. Matacotta, C. Taliani, and S. Barbanera, Solid State Commun. **122**, 181 (2002).
[3]Z. H. Xiong, D. Wu, Z. V. Vardeny, and J. Shi, Nature **427**, 821 (2004).
[4]T. S. Santos, J. S. Lee, P. Migdal, I. C. Lekshmi, B. Satpati, and J. S. Moodera, Phys. Rev. Lett. **98**, 016601 (2007).
[5]J. H. Shim, K. V. Raman, Y. J. Park, T. S. Santos, G. X. Miao, B. Satpati, and J. S. Moodera, Phys. Rev. Lett. **100**, 226603 (2008).
[6]V. A. Dediu, L. E. Hueso, I. Bergenti, and C. Taliani, Nat. Mater. **8**, 707 (2009).
[7]I. Bergenti, V. Dediu, M. Prezioso, and A. Riminucci, Philos. Trans. R. Soc. A **369**, 3054 (2011).
[8]K. V. Raman, S. M. Watson, J. H. Shim, J. A. Borchers, J. Chang, and J. S. Moodera, Phys. Rev. B **80**, 195212 (2009).
[9]G. Schmidt, D. Ferrand, L. W. Molenkamp, A. T. Filip, and B. J. van Wees, Phys. Rev. B **62**, R4790 (2000).
[10]M. Yunus, P. P. Ruden, and D. L. Smith, J. Appl. Phys. **103**, 103714 (2008).
[11]S. Sanvito, Nat. Phys. **6**, 562 (2010).
[12]J.-Y. Hong, Y.-M. Chang, C.-H. Chuang, K.-S. Li, Y.-C. Jhang, H.-W. Shiu, C.-H. Chen, W.-C. Chiang, and M.-T. Lin, J. Phys. Chem. C **116**, 21157 (2012).
[13]S. C. B. Mannsfeld, A. Virkar, C. Reese, M. F. Toney, and Z. Bao, Adv. Mater. **21**, 2294 (2009).
[14]Y. Q. Zhan, X. J. Liu, E. Carlegrim, F. H. Li, I. Bergenti, P. Graziosi, V. Dediu, and M. Fahlman, Appl. Phys. Lett. **94**, 053301 (2009).
[15]F. Borgatti, I. Bergenti, F. Bona, V. Dediu, A. Fondacaro, S. Huotari, G. Monaco, D. A. MacLaren, J. N. Chapman, and G. Panaccione, Appl. Phys. Lett. **96**, 043306 (2010).
[16]J. Cornil, D. Beljonne, J.-P. Calbert, and J.-L. Brédas, Adv. Mater. **13**, 1053 (2001).
[17]C. Dimitrakopoulos and P. Malenfant, Adv. Mater. **14**, 99 (2002).
[18]K.-S. Li, Y.-M. Chang, S. Agilan, J.-Y. Hong, J.-C. Tai, W.-C. Chiang, K. Fukutani, P. A. Dowben, and M.-T. Lin, Phys. Rev. B **83**, 172404 (2011).
[19]R. Hesse, T. Chassé, and R. Szargan, Fresenius J. Anal. Chem. **365**, 48 (1999).
[20]Y. Zou, L. Kilian, A. Schöll, T. Schmidt, R. Fink, and E. Umbach, Surf. Sci. **600**, 1240 (2006).
[21]W. Chen, H. Huang, S. Chen, L. Chen, H. L. Zhang, X. Y. Gao, and A. T. S. Wee, Appl. Phys. Lett. **91**, 114102 (2007).
[22]A. Schoell, Y. Zou, D. Huebner, S. G. Urquhart, T. Schmidt, R. Fink, and E. Umbach, J. Phys. Chem. **123**, 044509 (2005).
[23]J. Stöhr, *NEXAFS Spectroscopy* (Springer, New York, 1992).
[24]D. R. T. Zahn, G. N. Gavrila, and G. Salvan, Chem. Rev. **107**, 1161 (2007).
[25]J. Gustafsson, E. Moons, S. Widstrand, M. Gurnett, and L. Johansson, Surf. Sci. **572**, 32 (2004).
[26]Y. Hirose, A. Kahn, V. Aristov, P. Soukiassian, V. Bulovic, and S. R. Forrest, Phys. Rev. B **54**, 13748 (1996).